PHYSICAL REVIEW B **77**, 125133 (2008)

Analysis of surface-bulk screening competition in the electron-doped $Nd_{2-x}Ce_xCuO_4$ cuprate using x-ray photoemission spectroscopy

G. Panaccione,[1] F. Offi,[2] P. Torelli,[3,*] G. Vanko,[4,†] O. Tjernberg,[4,5] P. Lacovig,[6] A. Guarino,[7] A. Fondacaro,[4] A. Nigro,[7] M. Sacchi,[8] N. B. Brookes,[4] and G. Monaco[4]

[1]*TASC Laboratory, INFM, Area Science Park, S.S. 14 km 163.5, I-34012 Trieste, Italy*
[2]*CNISM and Dipartimento di Fisica, Università Roma Tre, Via della Vasca Navale 84, I-00146 Roma, Italy*
[3]*Laboratoire pour l'Utilisation du Rayonnement Electromagnetique LURE, Centre Universite Paris Sud, Boîte Postale 34, 91898 Orsay Cedex, France*
[4]*European Synchrotron Radiation Facility, Boîte Postale 220, F-38042 Grenoble Cedex 9, France*
[5]*LMSP, Royal Institute of Technology, Electrum 229, S-16440 Kista, Sweden*
[6]*Sincrotrone Trieste S.C.p.A., S.S. 14 km 163.5, Area Science Park, I-34012 Trieste, Italy*
[7]*CNR-INFM Laboratorio Regionale SuperMat Presso Dip di Fisica "E.R. Caianiello," Università degli Studi di Salerno, Via S. Allende, I-84081 Baronissi (SA), Italy*
[8]*Laboratoire de Chimie Physique Matière et Rayonnement, Universitè Pierre et Marie Curie, 75005 Paris, France and Synchrotron SOLEIL, Boîte Postale 48, 91192 Gif-Sur-Yvette, France*

(Received 14 January 2008; published 27 March 2008)

We report core level and valence band photoemission results obtained for $Nd_{2-x}Ce_xCuO_4$ ($x=0.15$) single crystals and films by using both soft and hard x rays, hence, with tunable depth sensitivity. When using hard x rays only, we observe distinct and energy separated structures in the main $2p^53d^9L$ peak of Cu $2p_{3/2}$ and $2p_{1/2}$ core levels, including the well screened features located at the high kinetic energy side, which were recently reported by Taguchi *et al.* [Phys. Rev. Lett. **95**, 177002 (2005)]. By varying the photoelectron takeoff angle, we analyze the difference in the screening properties between surface and bulk, and we demonstrate the depth dependence of the electronic properties by following the evolution of the bulk-related peak. The possible influence of the surface conditions on the Cu 2*p* spectral features is also discussed.

DOI: 10.1103/PhysRevB.77.125133 PACS number(s): 74.72.−h, 71.27.+a, 74.25.Jb

I. INTRODUCTION

Chemical doping is one of the main control parameters in the rich physics of cuprates. When charge carriers—holes or electrons—are introduced in the CuO planes, not only is superconductivity enabled, but the screening and/or correlation properties of the normal state are also severely modified. In the small class of *n*-doped cuprates, the manner in which the evolution from a Mott insulator to a metal occurs and the character of electronic states at the chemical potential have been intensively studied, but a coherent description of the underlying mechanism(s) is still lacking.[1] Although in both *n*-type and *p*-type cuprates the doping acts on the copper-oxygen plane, the location where the doping takes place introduces a major difference: the injection of carriers directly occurs in the Cu *d* orbitals when using electrons, while upon hole doping the carriers reside in the oxygen *p* orbitals.[2–4] This difference produces a variety of peculiar properties in the *n*-doped systems, such as a delicate balance of the electronic correlation already in the nonsuperconducting state.[4–6]

A direct access to the investigation of correlations in a solid is obtained by photoemission spectroscopy (PES), by which the presence of a core hole allows probing of the screening capability of the electrons. In cuprates with different Cu-O networks, Cu 2*p* PES line shapes have been able to reveal a complex valence structure via the analysis of satellites and of their relative intensities.[7–10] In the specific case of $Nd_{2-x}\cdot Ce_xCuO_{4+\delta}$ (NCCO)—the most representative compound within the electron-doped cuprates family[2]—PES results substantially contributed to the comprehension of the nature and location of the doping derived states in the insulating gap.[11–14]

However, the knowledge of electronic properties upon doping—and of their evolution—may be severely affected by surface effects. The relevance of depth sensitivity in NCCO has been recently raised by bulk sensitive PES results; e.g., a lower correlation at the surface has been proposed by soft x-ray valence band angular resolved photoemission spectroscopy (ARPES).[15] More surprisingly, independent experiments revealed that new peaks—the so-called shakedown satellites—appear on the low binding energy (BE) side of the Cu 2*p* main lines of NCCO only when bulk sensitivity is achieved.[16–20] It is important to underline that the presence of shakedown satellites on the low BE side of the *p* and *s* core levels in 3*d*-based transition metal oxides (TMOs) is not an exclusive feature of *n*-doped cuprates. Well screened peaks are observed in manganites and vanadates but only in the hard x-ray regime of PES (HAXPES),[18,19] whereas no extra feature has been observed in hole-doped cuprates so far.[20] These new findings not only raise questions on what PES signals can be considered representative of the bulk, but also suggest a possibly different screening mechanism between *n*- and *p*-doped TMOs. The origin and the assignment of these new features are under debate: recent results associate the new peaks, in both NCCO and Cr-doped V_2O_3, with the presence of a doping-induced band near the Fermi level E_F, holding a specific coherent spectral weight.[17,18] Such a scenario is supported in the specific case of V_2O_3, in which a correspondence between the satellite and the quasiparticle peak in the vicinity of the Fermi level has been observed,[21] but not in the case of bilayered manganites, in which no coherent intensity has been found near E_F.[22] Moreover, recent calculations have shown that nonlocal screening effects should be taken into account for a proper description of the process and that no specific coherent band is needed to explain the extraintensities in the Cu $2p$ core level of NCCO.[7,9,10,23,24]

In this work, we address these questions by tuning the bulk sensitivity with both soft x-ray and hard x-ray PES experiments on NCCO single crystals and films in their normal state. From the analysis of the Cu $2p_{3/2}$ and $2p_{1/2}$ core level line shapes over an extended photon energy range, we are able to identify the presence of surface and bulk screening channels by measuring the evolution of the Cu $2p$ satellite. By varying the photoelectron takeoff angle, angular dependent measurements on well characterized films allow us (i) to estimate how deep into the solid the surface modification of the electronic properties extends and (ii) to discuss the relationship between the Cu $2p$ line shapes and the surface conditions. Moreover, our HAXPES valence band data do not show any sizable coherent peak in the vicinity of the Fermi level, thus suggesting that the presence of extra satellites in NCCO core level spectra does not have the same origin as that in V_2O_3.

II. EXPERIMENTAL DETAILS

The $Nd_{1.85}Ce_{0.15}CuO_4$ single crystals were grown by the floating zone method. Unreduced samples from the same batch were fractured: one part was used for the PES experiment, while the other part was thermally treated and reduced, showing a critical superconducting temperature T_c of 21 K. The 900 nm thick films were grown by an "on-axis" dc sputtering technique on $SrTiO_3$ (001) substrates, with their c axis perpendicularly oriented to the surface plane. The crystal quality, the morphology, and the composition of the sample have been checked by high resolution x-ray diffraction, scanning electron microscopy (SEM), and energy dispersive spectroscopy. The surfaces of the films displayed an excess of Ce content ($x=0.16$). The films were not superconducting. Surface roughness has been evaluated by using a high resolution four circle diffractometer: identical values of less than 2 nm rms have been measured for both 250 and 500 nm thick films prior to the experiment, indicating that the roughness of the surface does not sizably increase with the thickness of the film. The roughness of the 900 nm sample has been measured after x-ray measurements, showing a maximum value of 15 nm over a 40×40 μm^2 area. SEM analysis on crystalline cleaved surfaces displays terraces of the order of 20/30 μm, separated by steps higher than 1 μm, which are uniformly distributed over the entire area of the sample (2×1 mm^2).

Experiments have been performed at the European Synchrotron Radiation Facility ESRF by using the Volume PhotoEmission (VOLPE) spectrometer (Ref. 25) for HAXPES (ID16 beamline, base vacuum of 9×10^{-10} mbar) and a Scienta SES-2002 for soft x-ray PES (ID08 beamline, base vacuum of 1×10^{-10} mbar). Spot size at normal emission geometry was 50×120 μm^2, and the overall energy resolution (beamline+analyzer) was set to 450 meV. The position of Fermi energy E_F and the overall energy resolution were estimated by measuring the metallic Fermi edge of a polycrystalline Au foil in thermal and electric contacts with the samples. Single crystals and films were cooled down to low temperature by a closed loop helium cryostat (the minimum temperature of the sample is 25 K). Cleaving on single crystal surfaces (room temperature or $T\approx 90$ K) has been performed in UHV by using a post that is glued to the surface, with the cleavage plane perpendicular to the c axis, whereas no surface treatment has been performed on the films prior to the HAXPES measurements. No signs of sample degradation and/or contamination and/or any variation of the PES signal due to photon exposure have been observed during the entire measurement period (up to 24 h for a cleaved surface in the HAXPES case). The same results have been consistently obtained on several cleaved samples.

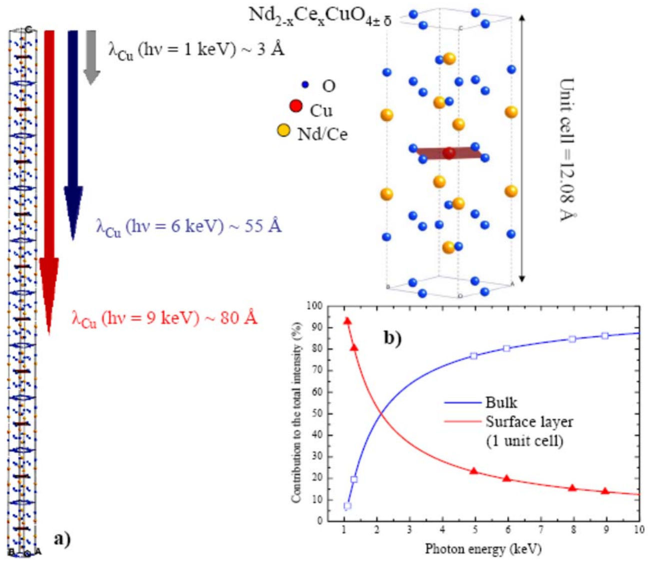

FIG. 1. (Color online) Crystal structure of $Nd_{1.85}Ce_{0.15}CuO_4$ and schematic of the probing depth achieved. The lines with arrows in (a) indicate the EAL λ as a function of the photon energy. As described in the text, the EAL is that of metallic Cu, i.e., $\lambda_{Cu}=0.093\,48E_k^{0.75}$, as experimentally determined at high energies (Ref. 26) and extrapolated by using the NIST code (Ref. 27). E_k is the kinetic energy of the measured peak. (b) shows the calculated bulk (blue curve) and surface (red curve) contributions to the total PES intensity as a function of the photon energy. The surface is defined as one unit cell of NCCO, i.e., 12.08 Å. The symbols denote the energy values used in our experiments.

Figure 1 describes the main ingredients of our bulk sensitive PES experiment, together with a sketch of the attained probing depth when $h\nu$ increases. Following experimental estimates[26] and theoretical calculations,[27] we calculated the effective attenuation length (EAL) λ of copper by the formula $\lambda_{Cu}=0.093\,48E_k^{0.75}$, where E_k is the kinetic energy of the measured peak. In our case, the Cu $2p_{3/2}$ core level has a BE of ≈930 eV; i.e., E_k is ≈100 eV at $h\nu=1$ keV, and λ_{Cu} is in the range of only a few angstroms [Fig. 1(a)]. Therefore, extreme surface sensitivity is expected in the soft x-ray measurements. Figure 1(b) shows the calculated bulk (blue

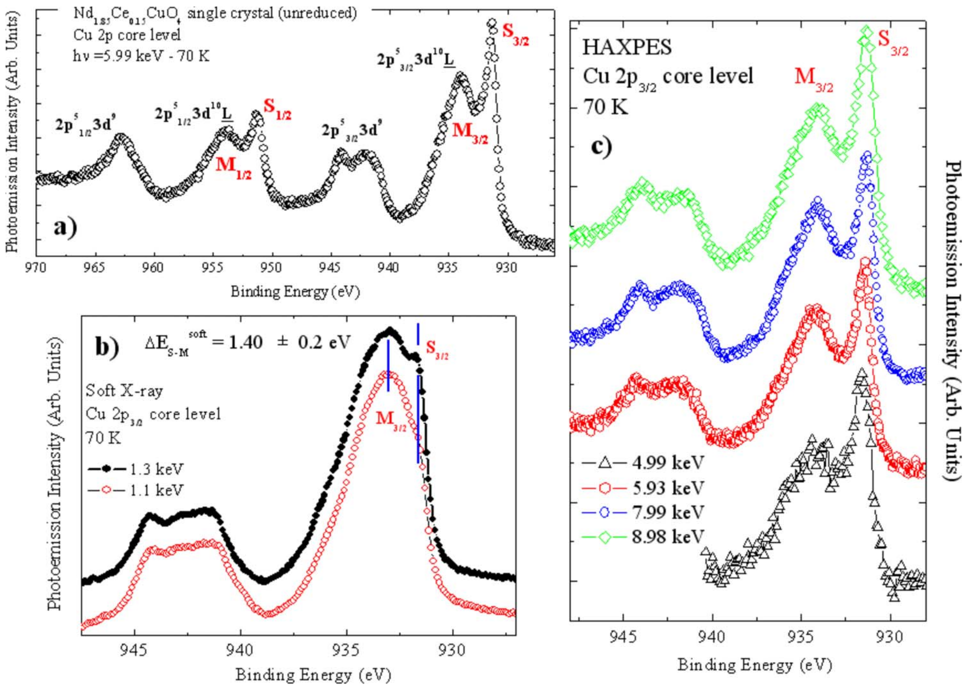

FIG. 2. (Color online) Cu $2p$ spectra of NCCO single crystals measured with soft and hard x rays. Surfaces have been cleaved at ≈90 K and measured at a low temperature (70 K) in a normal emission geometry. (a) shows a survey of the entire Cu $2p_{3/2}$+Cu $2p_{1/2}$ region measured at $h\nu$=5.99 keV, with the assignment of the final state configurations. (b) shows that the intense S feature is observed over a wide photon energy range. The bars in (c) indicate the weak S feature observed when using soft x rays. The spectra have been normalized to the same area after integral background subtraction.

curve) and surface (red curve) contributions to the total PES intensity as a function of photon energy. The surface is defined as one unit cell of NCCO, i.e., 12.08 Å. The symbols denote the energy values used in our experiments. At $h\nu$ =6 keV, λ_{Cu} is ≈55 Å and the bulk contribution is ≈80% of the total PES signal [Fig. 1(b)].

III. RESULTS AND DISCUSSION

In Fig. 2(a), we present a Cu $2p$ survey spectrum from an unreduced NCCO single crystal cleaved at low temperature (≈90 K) and measured at 70 K (panel a); in Figs. 2(b) and 2(c), we show the evolution of the Cu $2p_{3/2}$ spectral line shape as a function of photon energy. Both soft x-ray and HAXPES Cu $2p_{3/2}$ spectra are characterized by a poorly screened satellite at around 940–945 eV BE, with a $2p^53d^9$ character ($2p$ denotes a core hole). As probed with soft x rays [Fig. 2(b)], the Cu $2p_{3/2}$ main structure consists of (i) a broad peak identified as $2p^53d^{10}L$ (with L indicating a ligand hole),[8,14] (ii) an additional feature on the low BE side evolving from a shoulder to a weak peak when $h\nu$ increases, where their energy separation is $\Delta E_{soft}=1.4\pm0.2$ eV. HAXPES spectra [Fig. 2(c)] display a remarkably different structure: two intense peaks are observed (labeled as S and M, $\Delta E_{hard}=2.8\pm0.1$ eV), and identical features are found in the Cu $2p_{1/2}$ peak [Fig. 2(a)]. As from Fig. 2(c), the energy separation ΔE_{hard} between the satellite S and the main peak M does not vary over an extended photon energy range (from $h\nu\approx5$ keV to $h\nu\approx9$ keV), i.e., varying the EAL from ≈40 Å to ≈80 Å (see Fig. 1), thus allowing us to safely consider HAXPES spectra as representatives of the bulk. In Fig. 3, we compare soft x-ray and HAXPES Cu $2p_{3/2}$ spectra. After integral background subtraction, the spectra have been normalized to the same area under the entire $2p_{3/2}$ energy range ($2p^53d^9+2p^53d^{10}L+S$ satellite) in order to fulfill the conservation of the number of electrons in a shell.[28] It is important to underline that a proper normalization can be obtained only when considering the intensity of the $2p^53d^9$ poorly screened satellite as a reference due to its insensitivity

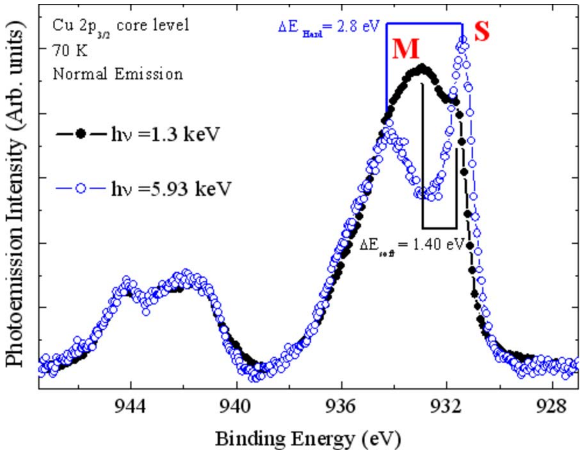

FIG. 3. (Color online) Comparison of soft-x-ray and HAXPES Cu $2p_{3/2}$ spectra. The energy separation between S and M is labeled as $\Delta E_{soft}=1.4\pm0.2$ eV and $\Delta E_{hard}=2.8\pm0.1$ eV.

to different experimental conditions and its agreement with theoretical predictions.[29] The difference between ΔE_{hard} and ΔE_{soft} is due mainly to the energy location of peak *M*, which is in fair agreement with previous results obtained from reduced (superconducting) NCCO crystals.[12,16,17]

After ascertaining the bulk nature of the *S* satellite peak, we address its origin and final state assignment in the following. Theoretical and experimental results for *n*-doped cuprates suggest that (i) a link between the intensity of the low BE satellite and the doping is expected[7,17] and (ii) the $3d^{10}$ configuration is distinct in energy (lower BE) with respect to those of the Cu $2p$. In fact, extra carriers are expected to go to the Cu sites, changing their electronic configuration from $3d^9$ to $3d^{10}$, as suggested by the appearance of a distinct structure on the low BE side of the main $2p^5 3d^{10}L$ peak upon electron doping of Nd_2CuO_4.[11,12] As discussed in Sec. I, the presence of a coherent band responsible for the *S* satellite has also been proposed in NCCO.[17] A direct method to detect the relationship between satellite peaks in the core level and electronic states near E_F is the measurement of valence band PES. Valence band spectra obtained with both soft and hard x rays are presented in Fig. 4. By taking into account the different p/d cross section ratios when passing from soft to hard x rays,[30–32] the main structures of the oxygen band are recognizable, as indicated by the arrows. In the inset, a detailed view of the PES intensity in the vicinity of E_F is presented, as measured with two photon energies. Although a fine analysis of the states near the chemical potential is limited by the present energy resolution (0.4 eV) in the HAXPES spectra, the spectral weight, if any, of a new coherent band is under the detection limit in both HAXPES and soft-x-ray data. Within our sensitivity, the results in Figs. 2–4 (i) do not support a clear connection between the *S* satellite and the quasiparticle or coherent features in NCCO, which is contrary to what was observed in V_2O_3 (Ref. 21), and (ii) do not show a sizable increase in the coherent weight near E_F when achieving bulk sensitivity with high photon energies (also observed for V_2O_3). Moreover, our results indicate that the appearance of the satellite *S* does not depend on the subtle apical and/or interstitial oxygen stoichiometry, our samples being unreduced, and clearly points to a competition between surface and bulk characters within the Cu-O planes, involving the oxygen ligand.

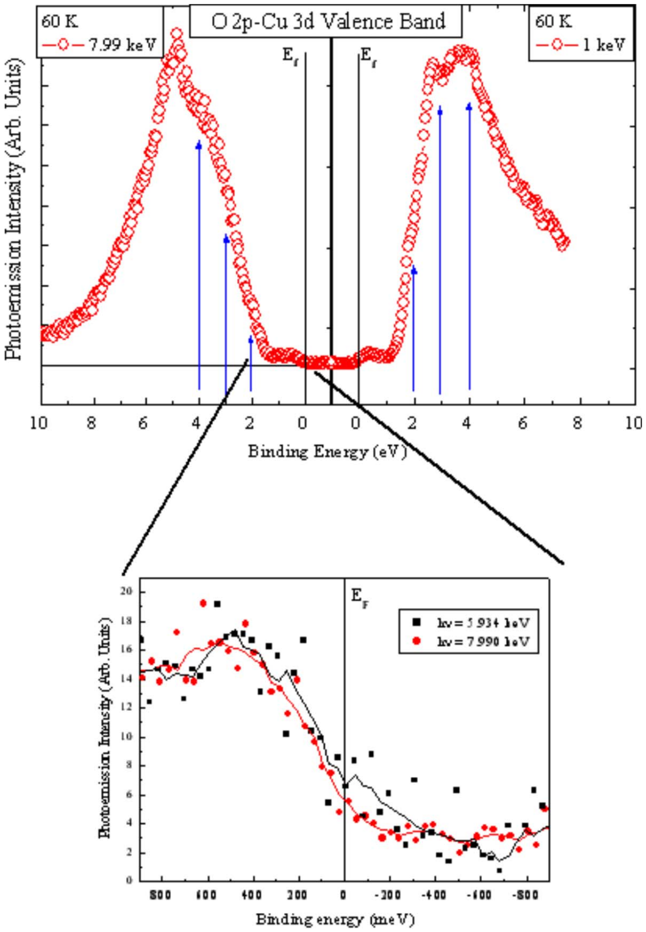

FIG. 4. (Color online) Comparison between hard (left panel) and soft (right panel) x-ray valence band spectra of cleaved NCCO single crystals. Inset: detailed view of the PES intensity near E_F at two photon energies in the HAXPES regime (the black square and red circles represent experimental data; the lines denote smoothing of experimental data). No evidence of a coherent intensity in the vicinity of the Fermi level is found in both HAXPES and soft-x-ray data.

To further substantiate the change in the electron screening channels when passing from the bulk to the surface, we have measured the HAXPES of Cu $2p_{3/2}$ vs the photoelectron takeoff angle in order to enhance the surface contribution.[16,19] In such angular dependent measurements, surface flatness is of utmost importance,[11,33] and the presence of terraces separated by steps as high as 1 μm prevents a precise analysis of angular dependent results for cleaved crystalline surfaces. To minimize the sources of errors, we performed a takeoff angle dependent PES on a NCCO thick film (900 nm) without any surface treatment to preserve its original surface roughness. The results are presented in Fig. 5: the evolution of the intensities of peaks *S* and *M* in Fig. 5(b) confirms the changes in the screening properties between the surface and the bulk. At grazing takeoff angles, when surface contribution is predominant, the intensity of the *S* peak is reduced and ΔE decreases, leading to a line shape remarkably similar to the soft-x-ray one. The attenuation of a bulk peak covered by an overlayer can be described by the formula $I(\varphi)=I_0 \exp(d/\lambda)([(\cos\varphi)-1]/\cos\varphi)$, where $I_0=1$ is the intensity without the overlayer, *d* is the thickness of the overlayer, λ is the EAL, and φ is the angle between the photoelectron direction and the surface normal (see the geometrical scheme in the inset). In Fig. 5(a), the lines are calculations of the exponential attenuation of a bulk signal covered by an overlayer of thickness *t* (with EAL $\lambda=55$ Å), i.e., assuming a surface layer with no *S* peak. Experimental data are compatible with a $t_{surf}=15\pm5$ Å, i.e., less than two unit cells in NCCO. The results in Fig. 5 give direct evidence that both the line shape and energy location of Cu $2p$ peaks are severely modified in the topmost layers. In the case of the film, the surface layer does not display the *S* satellite because of an altered composition with respect to the bulk layer due to the direct exposure to air and to the absence of surface preparation. Similarly, the surface of a crystal cleaved *in situ* does not display the *S* feature as a result of the different electronic environment in the first layers(s).

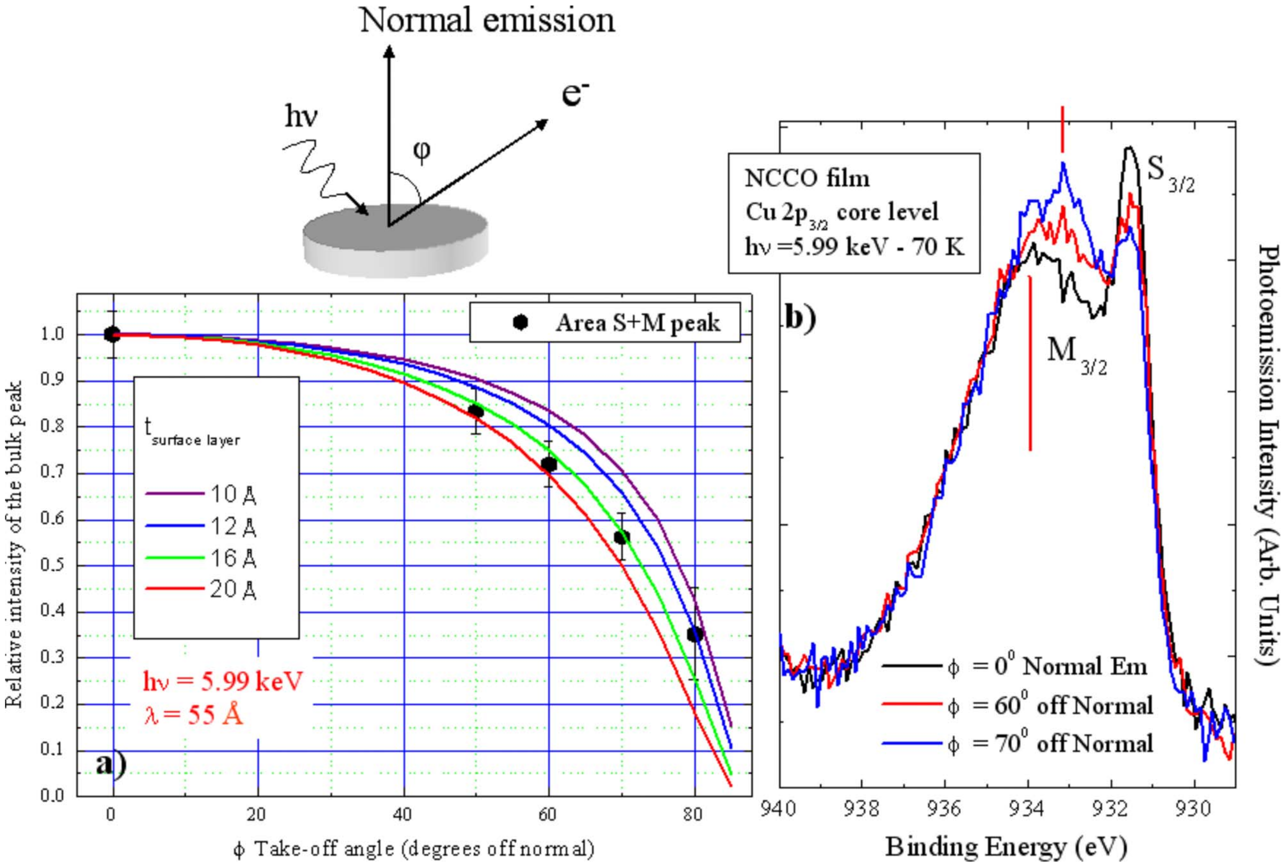

FIG. 5. (Color online) Angular dependent HAXPES spectra of a NCCO film and estimate of the attenuation due to the surface layer. (a) Evolution of the bulk peak area measured at $h\nu = 5.99$ keV vs the takeoff angle, following the experimental geometry sketched in the inset. The maximum intensity ($I = 1$) corresponds to normal emission. The area of peak $S+M$ (filled circles with error bars) is shown with the attenuation curves calculated with λ_{Cu}, assuming a surface layer of thickness t_{surf} with no peak S. Experimental data are compatible with a $t_{surf} = 15 \pm 5$ Å. (b) Cu $2p_{3/2}$ spectra of the NCCO film at selected takeoff angles. The intensity of peak S decreases, and M peak spectral weight shifts to a lower BE; the shift in the BE of the M peak is ≈ 0.8 eV, as indicated by the vertical lines. The blue spectrum ($\varphi = 70°$ off normal) reproduces the line shape of the soft-x-ray spectra well in Figs. 1 and 2. The spectra are normalized to the same area.

The influence of surface conditions on the Cu $2p$ line shape is addressed in Fig. 6. When samples are cleaved at low temperatures (<90 K), the energy location, the overall line shape, and the energy separation in both Cu $2p_{3/2}$ and $2p_{1/2}$ peaks do not vary vs photon energy (from 5 to 9 keV), thermal cycling (from 90 to 20 K and from 20 to 300 K), and time (24 h after cleaving). However, we observe a different intensity of the S satellite in a few specific locations of the sample, a result that is compatible with the presence of doping inhomogeneities (both in the volume and at the surface) and coherent with the picture of a direct link between electron doping and the intensity of the S satellite. A room temperature cleave leads to a sizable change in the $2p^5 3d^{10} L$ peak, including the S satellite, with a filling of the valley between peaks S and M, whereas the poorly screened $2p^5 3d^9$ feature at higher binding energies is fairly insensitive to the surface conditions.[29]

Our spectral shape analysis suggests that changes in the electronic structure occur at the surface via (i) a competition between local and nonlocal screening channels, affecting only the intensity of the S and M peaks, and (ii) a distinct charge-transfer energy in the vicinity of the surface, producing (as a function of the surface conditions) both a different BE of the M peak and a weakening of the S feature.[17,21] Recent theoretical results indicate a clear relationship between the charge-transfer energy in the presence of a core hole and (a) the relative energy distance of $2p^5 3d^{10} L$ and $2p^5 3d^{10}$ peaks and (b) a variation in the intensity of the $2p^5 3d^9$ satellite.[7] Our results only partially confirm this interpretation since the $2p^5 3d^9$ line shape remains unchanged in the experimental data. Moreover, the observed differences may have a common origin involving the charge balance in the crystal planes. The cleave of NCCO produces a polar surface with a redistribution of the charge (self-doping effect) and a possible change in covalency between Cu and O ligands within, at least, the first unit cell.

IV. CONCLUSIONS

In summary, by performing PES experiments on NCCO with variable probing depths, we reveal a richer variety of screening channels than what was previously believed in a prototypical electron-doped cuprate, and we explore the influence of the surface on the electronic properties. A com-

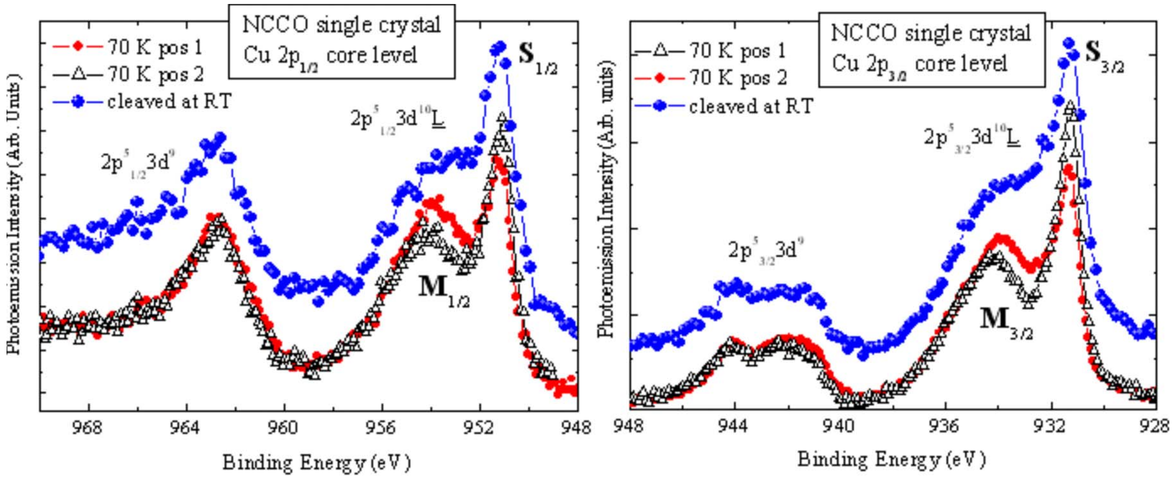

FIG. 6. (Color online) *S* and *M* peak line shapes in the HAXPES regime for different surface conditions. The spectra have been normalized to the same area and measured at normal emission. Although the energy locations of *S* and *M* peaks do not vary, both in the $2p_{1/2}$ (left panel) and $2p_{3/2}$ regions (right panel), the *S* intensity changes when changing the position of the spot on the sample. The blue curve, corresponding to the room temperature cleave, reveals a drastic change in both ratio and line shape. The poorly screened $2p^53d^9$ feature is unchanged.

parison between experimental data and calculated effective attenuation lengths allows us to set an estimate in the change in screening properties; i.e., the difference between surface and bulk screening is located within two unit cells of NCCO. Assuming that (a) the extra peak disappears due to the change in the electronic properties at the surface and (b) the extra peak represents another channel to be taken into account, our results open important questions regarding the difference between *n*-doped and *p*-doped cuprates and call for further theoretical and experimental efforts to elucidate the delicate equilibrium of electronic correlation in transition metal oxides.

ACKNOWLEDGMENTS

We acknowledge fruitful discussions with A. Damascelli, C. Hague, P. Postorino, A. Vecchione, and G. A. Sawatzky. This work was supported by Istituto Nazionale per la Fisica della Materia–CNR (INFM-CNR). Thanks are due to R. Claessen and S. Hossain for ideas and contribution related to Fig. 1, to C. Veenstra, J. Rosen, and R. Wicks for help in data analysis, to V. Grillo for SEM data acquisition, to M. Lazzarino for AFM experiments, and to M. Månsson and T. Claesson for assistance with the soft-x-ray measurements.

---

[*] Present address: S3, CNR-INFM, Via G. Campi 213/A, I-41100 Modena, Italy.

[†] Present address: KFKI Research Institute for Particle and Nuclear Physics, H-1525 Budapest, P.O.B. 49, Hungary.

[1] M. Imada, A. Fujimori, and Y. Tokura, Rev. Mod. Phys. **70**, 1039 (1998).

[2] Y. Tokura, H. Takagi, and S. Uchida, Nature (London) **337**, 345 (1989).

[3] N. P. Armitage, F. Ronning, D. H. Lu, C. Kim, A. Damascelli, K. M. Shen, D. L. Feng, H. Eisaki, Z.-X. Shen, P. K. Mang, N. Kaneko, M. Greven, Y. Onose, Y. Taguchi, and Y. Tokura, Phys. Rev. Lett. **88**, 257001 (2002).

[4] J. M. Tranquada, S. M. Heald, A. R. Moodenbaugh, G. Liang, and M. Croft, Nature (London) **337**, 720 (1989).

[5] P. K. Mang, O. P. Vajk, A. Arvanitaki, J. W. Lynn, and M. Greven, Phys. Rev. Lett. **93**, 027002 (2004).

[6] A. Koitzsch, J. Fink, M. S. Golden, K. Karlsson, O. Jepsen, O. Gunnarsson, L. L. Miller, H. Eisaki, S. Uchida, G. Yang, and S. Abell, Phys. Rev. B **66**, 024519 (2002).

[7] K. Okada and A. Kotani, J. Phys. Soc. Jpn. **74**, 653 (2005).

[8] K. Karlsson, O. Gunnarsson, and O. Jepsen, Phys. Rev. Lett. **82**, 3528 (1999).

[9] M. A. van Veenendaal, G. A. Sawatzky, and W. A. Groen, Phys. Rev. B **49**, 1407 (1994).

[10] M. van Veenendaal, Phys. Rev. B **74**, 085118 (2006).

[11] T. Suzuki, M. Nagoshi, Y. Fukuda, K. Oh-ishi, Y. Syono, and M. Tachiki, Phys. Rev. B **42**, 4263 (1990).

[12] P. G. Steeneken, L. H. Tjeng, G. A. Sawatzky, A. Tanaka, O. Tjernberg, G. Ghiringhelli, N. B. Brookes, A. A. Nugroho, and A. A. Menovsky, Phys. Rev. Lett. **90**, 247005 (2003).

[13] N. Harima, J. Matsuno, A. Fujimori, Y. Onose, Y. Taguchi, and Y. Tokura, Phys. Rev. B **64**, 220507(R) (2001).

[14] J. W. Allen, C. G. Olson, M. B. Maple, J.-S. Kang, L. Z. Liu, J.-H. Park, R. O. Anderson, W. P. Ellis, J. T. Markert, Y. Dalichaouch, and R. Liu, Phys. Rev. Lett. **64**, 595 (1990).

[15] T. Claesson, M. Månsson, C. Dallera, F. Venturini, C. De Nadaï, N. B. Brookes, and O. Tjernberg, Phys. Rev. Lett. **93**, 136402 (2004).

[16] M. Tsunekawa, A. Sekiyama, S. Kasai, A. Yamasaki, H. Fujiwara, M. Sing, A. Shigemoto, S. Imada, Y. Onose, Y. Tokura, T. Muro, and S. Suga, J. Electron Spectrosc. Relat. Phenom. **144–147**, 541 (2005).

[17] M. Taguchi, A. Chainani, K. Horiba, Y. Takata, M. Yabashi, K. Tamasaku, Y. Nishino, D. Miwa, T. Ishikawa, T. Takeuchi, K. Yamamoto, M. Matsunami, S. Shin, T. Yokoya, E. Ikenaga, K. Kobayashi, T. Mochiku, K. Hirata, J. Hori, K. Ishii, F. Nakamura, and T. Suzuki, Phys. Rev. Lett. **95**, 177002 (2005).

[18] M. Taguchi, A. Chainani, N. Kamakura, K. Horiba, Y. Takata, M. Yabashi, K. Tamasaku, Y. Nishino, D. Miwa, T. Ishikawa, S. Shin, E. Ikenaga, T. Yokoya, K. Kobayashi, T. Mochiku, K. Hirata, and K. Motoya, Phys. Rev. B **71**, 155102 (2005).

[19] K. Horiba, M. Taguchi, A. Chainani, Y. Takata, E. Ikenaga, D. Miwa, Y. Nishino, K. Tamasaku, M. Awaji, A. Takeuchi, M. Yabashi, H. Namatame, M. Taniguchi, H. Kumigashira, M. Oshima, M. Lippmaa, M. Kawasaki, H. Koinuma, K. Kobayashi, T. Ishikawa, and S. Shin, Phys. Rev. Lett. **93**, 236401 (2004).

[20] M. Taguchi, A. Chainani, N. Kamakura, K. Horiba, Y. Takata, M. Yabashi, K. Tamasaku, Y. Nishino, D. Miwa, T. Ishikawa, S. Shin, E. Ikenaga, T. Yokoya, K. Kobayashi, T. Mochiku, K. Hirata, and K. Motoya, Phys. Rev. B **76**, 169901(E) (2007); M. Taguchi, M. Matsunami, A. Chainani, K. Horiba, Y. Takata, K. Yamamoto, R. Eguchi, M. Yabashi, K. Tamasaku, Y. Nishino, T. Nishio, H. Uwe, T. Mochiku, K. Hirata, J. Hori, K. Ishii, F. Nakamura, T. Suzuki, S. Shin, and T. Ishikawa, arXiv:cond-mat/0612676 (unpublished).

[21] G. Panaccione, M. Altarelli, A. Fondacaro, A. Georges, S. Huotari, P. Lacovig, A. Lichtenstein, P. Metcalf, G. Monaco, F. Offi, L. Paolasini, A. Poteryaev, M. Sacchi, and O. Tjernberg, Phys. Rev. Lett. **97**, 116401 (2006).

[22] F. Offi, P. Torelli, M. Sacchi, P. Lacovig, A. Fondacaro, G. Paolicelli, S. Huotari, G. Monaco, C. S. Fadley, J. F. Mitchell, G. Stefani, and G. Panaccione, Phys. Rev. B **75**, 014422 (2007).

[23] K. Okada and A. Kotani, Phys. Rev. B **52**, 4794 (1995).

[24] M. A. van Veenendaal and G. A. Sawatzky, Phys. Rev. Lett. **70**, 2459 (1993).

[25] P. Torelli, G. Cautero, M. Cautero, A. Fondacaro, M. Grioni, B. Krastanov, P. Lacovig, G. Monaco, F. Offi, G. Paolicelli, M. Sacchi, G. Stefani, R. Tommasini, R. Verbeni, and G. Panaccione, Rev. Sci. Instrum. **76**, 023909 (2005).

[26] M. Sacchi, F. Offi, P. Torelli, A. Fondacaro, C. Spezzani, M. Cautero, G. Cautero, S. Huotari, M. Grioni, R. Delaunay, M. Fabrizioli, G. Vankó, G. Monaco, G. Paolicelli, G. Stefani, and G. Panaccione, Phys. Rev. B **71**, 155117 (2005).

[27] NIST Electron Inelastic-Mean-Free-Path database, Version 1.1, National Institute of Standard and Technology, U.S., 2000.

[28] The error introduced in the normalization to the same area by the integral background subtraction is $<5\%$.

[29] G. van der Laan, C. Westra, C. Haas, and G. A. Sawatzky, Phys. Rev. B **23**, 4369 (1981).

[30] J. J. Yeh and I. Lindau, At. Data Nucl. Data Tables **32**, 1 (1985).

[31] J. H. Scofield, LLNL Report No. UCRL-51326, 1973 (unpublished).

[32] G. Panaccione, G. Cautero, M. Cautero, A. Fondacaro, M. Grioni, P. Lacovig, G. Monaco, F. Offi, G. Paolicelli, M. Sacchi, N. Stojic, G. Stefani, R. Tommasini, and P. Torelli, J. Phys.: Condens. Matter **17**, 2671 (2005).

[33] G. H. Kwei, S.-W. Cheong, Z. Fisk, F. H. Garzon, J. A. Goldstone, and J. D. Thompson, Phys. Rev. B **40**, 9370 (1989).